6. Quinones in PSI

The crystal structure of PSI from *T. elongatus* at 2.5 Å resolution (Jordan et al., 2001) solved the riddle of the microscopic structure of this protein-pigment complex located in the thylakoid membrane.

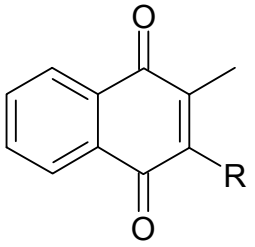

Figure 6-0-1. Phylloquinone. **R** stands for non-redox active part of aliphatic chain.

Based on measurements of the triplet yield of P700, $E_m(A_1)$ was estimated to be relatively low, with the value of ~–800 mV (Sétif et al., 1990). This extremely negative value was widely accepted, since its electron acceptor F_X was known to have a relatively low E_m value of ~–650-–670 mV (Parrett et al., 1989; Semenov et al., 2000; Shinkarev et al., 2000). Iwaki and Itoh estimated that $E_m(A_1)$ was 50-80 mV more negative than $E_m(F_X)$ (Iwaki and Itoh, 1994). These values of $E_m(A_1)$ and $E_m(F_X)$ yield an energetically downhill (i.e. exergonic) reaction for the ET from A_1 to F_X. Recently, $E_m(A_1)$ was measured to be –540 mV for PSI from spinach with voltammetry (Munge et al., 2003). In contrast to the former estimations, this value is considerably high.

6.1. Native PSI protein-pigment complex

6.1.1. Calculated $E_m(A_1)$ in native PSI

We calculate $E_m(A_{1A})$ and $E_m(A_{1B})$ to be –531 mV and –686 mV, respectively (Ishikita and Knapp, 2003). In the presence of all crystal waters, we obtain more negative values for $E_m(A_1)$ of –629 mV for A_{1A} and –776 mV for A_{1B}. But, these values may contain an uncertainty of the hydrogen positions of the water molecules.

The calculated $E_m(A_{1A})$, which is by 119 - 139 mV higher than measured $E_m(F_X)$ of ~–650 - –670 mV (Parrett et al., 1989; Semenov et al., 2000; Shinkarev et al., 2000), implies that the radical state A_1^- observed in EPR spectroscopy (Bittl et al., 1997) should refer to A_{1A}. Our assignment of the radical state to A_{1A} is also in agreement with conclusion of the mutagenesis studies (Yang et al., 1998). On the other hand, the calculated $E_m(A_{1B})$ indicates that the ET reaction from A_{1B} to F_X is weakly exergonic (driving energy of 16 - 36 meV).

In general, time resolved optical spectra for forward ET from A_1 to F_X are biphasic, which may be due to the co-existence of a fast ET on the B-branch and a slow ET on the A-branch (Guergova-Kuras et al., 2001; Gong et al., 2003; Xu et al., 2003b; Xu et al., 2003a). Recently, Agalarov and Brettel investigated temperature dependence of the two phases, and determined activation energies to be 110 mV for the slower phase and 15 mV for the faster phase (Agalarov and Brettel, 2003). This is in perfect agreement with our calculated Em difference between A_1 and F_X i.e., endergonic by 119 - 139 meV for A_{1A} but of exergonic by 16 - 36 meV for A_{1B} (Ishikita and Knapp, 2003).

6.1.2. Kinetics of ET from A_1^- to F_X in native PSI: a single or double branch ET activity?

The lifetime ($t_{1/e} = 1/k^{ET}$) of the reduced state A_1^- is limited by ET processes. It has been established that ET from A_1^- to F_X is biphasic, the slower phase being 206 - 355 ns, and the faster phase being 10 - 36 ns (Brettel, 1988; Sétif and Brettel, 1993; Leibl et al., 1995; Yang et al., 1998; Joliot and Joliot, 1999; Guergova-Kuras et al., 2001; Purton et al., 2001). Mutational studies of either Trp-A697 or Trp-B673 to Phe near A_{1A}/A_{1B} suggested that the slower/faster phases originates from the forward ET from A_{1A}/A_{1B} to F_X (Guergova-Kuras et al., 2001; Gong et al., 2003; Xu et al., 2003b; Xu et al., 2003a) (see Figure 1-3).

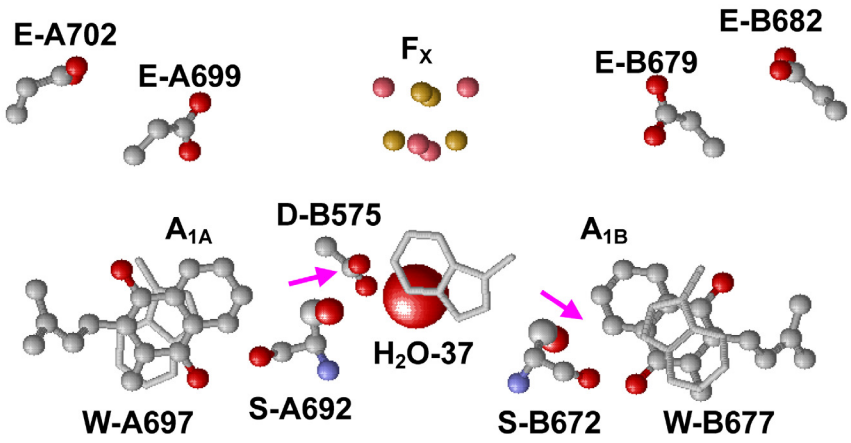

Figure 6-1-1. Quinone binding site in PSI. Trp are depicted as stick model. The orientation of backbone carbonyl group at Ser-A692 and Ser-B672 are indicated with pink arrow.

Based on calculated $E_m(A_{1A/B})$ and the kinetic equation of Page et al. (Page et al., 1999) , we obtained $t_{1/e}$ = 220 - 375 ns from the E_m difference between A_{1A} and F_X and $t_{1/e}$ = 6 - 8 ns from the E_m difference between A_{1B} and F_X (Ishikita and Knapp, 2003), in agreement with the assignment in the mutational study (Guergova-Kuras et al., 2001). These estimates for the A_1^- lifetime were obtained by using a reorganization energy of λ = 1.0 estimated from the kinetics of ET from A_1 to F_X (Schlodder et al., 1998).

Time-resolved EPR spectroscopy identified the appearance of the radical state A_1^- for only a single quinone (Bittl et al., 1998; Yang et al., 1998). Thus, it was proposed that the ET from A_1 to F_X occurs only in a single ET branch, presumably A-branch. Apparently, this is in contradiction to the interpretation derived from kinetic studies as both branches being ET-active (Brettel, 1988; Sétif and Brettel, 1993; Leibl et al., 1995; Yang et al., 1998; Joliot and Joliot, 1999; Guergova-Kuras et al., 2001; Purton et al., 2001). However, it should be noted that the time-resolved EPR measurements were sensitive only for times longer than a ~50 ns such that a faster phase observed in UV/VIS spectroscopic studies could be not detected (Zech et al., 2000).

Thus, we concluded that (i) both branches are ET active, (ii) the E_m difference of 155 mV between A_{1A} and A_{1B} leads to a biphasic ET process, and that (iii) the ET from A_1 to F_X is faster in the B-branch than the A-branch.

6.1.3. Difference between $E_m(A_{1A})$ and $E_m(A_{1B})$.

The calculated $E_m(A_{1A})$ and $E_m(A_{1B})$ differ by 155 mV (Ishikita and Knapp, 2003). F_X is a cofactor that significantly down-shifts $E_m(A_{1A/B})$ by ~240 - 260 mV, but its influence on $E_m(A_{1A})$ and $E_m(A_{1B})$ is essentially the same (edge-to-edge distances for F_X – A_{1A} and F_X – A_{1B} are identically 6.8 Å) (Ishikita and Knapp, 2003). Similarly, F_A and

F_B do not essentially differentiate between $E_m(A_{1A})$ and $E_m(A_{1B})$ in spite of their asymmetrical positions with respect to pseudo-C_2 axis (Ishikita and Knapp, 2003) (see also figure 1-3).

We found that the E_m difference between A_{1A} and A_{1B} is mainly attributable to the following two factors; (i) protonation state of Asp-B575. This residue is closer to A_{1A} than to A_{1B} (minimum O – O distance with A_{1A} and A_{1B} of 8.9 Å and 13.7 Å, respectively, Figure 6-1-1). Its protonation state is more strongly coupled to the formation of A_{1A}^- than that of A_{1B}^- (ii) the backbone orientation of PsaA and PsaB. Especially, the backbone carbonyl group stabilizes A_{1A}^- and A_{1B}^- by different amounts, namely due to the difference in the backbone orientation of Ser-A692 and Ser-B672 (Figure 6-1-1).

A) Asp-B575. The symmetry counterpart to Asp-B575 in subunit PsaB is the non-titratable residue Gln-A588. Furthermore, in our computation, Asp-B575 is the only residue that changes its protonation state most significantly upon formation of $A_{1A/B}^-$ state (Ishikita and Knapp, 2003). Asp-B575 becomes protonated by 0.85 H^+ and 0.17 H^+ upon formation of A_{1A}^- and A_{1B}^- states, respectively, while fully ionized in the $A_{1A}^0A_{1B}^0$ state. This yields that Asp-B575 is protonated by 0.44 H^+ and 0.09 H^+ when $E_m(A_{1A})$ and $E_m(A_{1B})$ are measured, respectively (i.e. when $[A_{1A}] = [A_{1A}^-]$ or $[A_{1B}] = [A_{1B}^-]$). This difference of the protonation of Asp-B575 yields a net E_m difference of 82 mV between $E_m(A_{1A})$ and $E_m(A_{1B})$ (Ishikita and Knapp, 2003).

B) Backbone carbonyl group of Ser-A692 and Ser-B672. We found a different orientation of the backbone carbonyl group between Ser-A692 and Ser-B672 (O_{A1} – $O_{Ser\text{-}backbone}$ distance 6.2 Å/ 4.0 Å for $A_{1A/B}$, Figure 6-1-1). The backbone charges of the symmetry equivalent pair of residues Ser-A692 and Ser-B672 yield a up-shift of 17 mV in the $E_m(A_{1A})$ and a down-shift of 48 mV in $E_m(A_{1B})$, which yields a net E_m difference of 65 mV between A_{1A} and A_{1B}.

Mutation of Ser-A692 to Cys resulted in a 5 % decrease in the hyperfine coupling of the methyl group of the A_1 ring, while mutation of Ser-B682 to Cys did not affect the shape of the spectra (Xu et al., 2003b; Xu et al., 2003a). However, such mutational studies may not be able to assess the effect of the backbone orientation of the corresponding carbonyl groups, unless the backbone conformation is changed in a controlled fashion.

The different orientations of the carbonyl groups of Ser-A692 and Ser-B672 may be related to the location of a crystal water molecule (HOH-132), which is at an H-bond distance from Ser-A692 (O – O distance 2.9 Å). No corresponding crystal water is found near Ser-B672 (Jordan et al., 2001).

Conclusion:

We calculate $E_m(A_{1A})$ and $E_m(A_{1B})$ to be –531 mV and –686 mV, respectively. It has been established that ET from A_1^- to F_X is biphasic, the slower phase being 206 to 355 ns, and the faster phase being 10 to 36 ns (Brettel, 1988; Sétif and Brettel, 1993; Leibl et al., 1995; Yang et al., 1998; Joliot and Joliot, 1999; Guergova-Kuras et al., 2001; Purton et al., 2001). Based on calculated $E_m(A_{1A/B})$ and the kinetic equation of Page et al. (Page et al., 1999), **we obtained $t_{1/e}$ = 220 - 375 ns from the E_m difference between A_{1A} and F_X and $t_{1/e}$ = 6 - 8 ns from the E_m difference between A_{1B} and F_X (Ishikita and Knapp, 2003).**

6.2. P700-F_X core

6.2.1. P700-F_X core treatment

Subunit PsaC of PSI is largely similar to ferredoxins that contain two Fe_4S_4 centers. To test the functional role of this subunit, a PSI mutant lacking subunit PsaC (P700-F_X core) has been studied. A consequence of the P700-F_X core preparation is not only the absence of PsaC, which contains the two iron-sulfur clusters F_A and F_B, but also the lack of PsaD and PsaE; these two subunits are in close contact with PsaC and bind to PsaA/PsaB only after PsaC is bound.

A P700-F_X core can be generated either chemically (i) by urea treatment (urea treated PSI) (Golbeck et al., 1988; Parrett et al., 1989; Golbeck, 2003; Gong et al., 2003) or genetically in two ways by deleting (ii) the *psaC* gene (*psaC*$^-$ PSI) (Yu et al., 1995; Golbeck, 2003), or (iii) the *rub*A gene (*rub*A$^-$ PSI) (Shen et al., 2002b; Shen et al., 2002a). The latter leads to a P700-F_X core in which F_X is initially absent but can be later reconstituted. If not otherwise specified, we name all three differently generated incomplete PSI protein complexes "P700-F_X cores" in the present study. In spite of the deletion of the subunit PsaC in the neighborhood of F_X, the measured ET rate from A_1 to F_X remains essentially unchanged (180 ns by UV-VIS (Lüneberg et al., 1994) or 190 ns by EPR (van der Est et al., 1994) in urea treated PSI) relative to the native PSI complex, where the corresponding time constant was between 206 ns and 355 ns (Brettel, 1988; Sétif and Brettel, 1993; Leibl et al., 1995; Joliot and Joliot, 1999; Guergova-Kuras et al., 2001; Purton et al., 2001). Note that urea treatment could be accompanied with a partial (10 % (Golbeck et al., 1988) or 30% (van der Est et al., 1994)) loss of F_X with respect to the native PSI complex. With F_X absent, ET cannot proceed past A_1.

$E_m(A_{1A})$ and $E_m(A_{1B})$ are calculated to be –545 mV and –652 mV, respectively in the P700-F_X core (Ishikita et al., 2006). Although these values are similar to the calculated $E_m(A_1)$ in the native PSI complex ($E_m(A_{1A})$ = –531 mV; $E_m(A_{1B})$ = –686 mV (Ishikita and Knapp, 2003)), the shift in $E_m(A_{1B})$ is slightly larger than that in $E_m(A_{1A})$. As a consequence, the asymmetry in the $E_m(A_{1A/B})$ values decreases from 155 mV (Ishikita and Knapp, 2003) in the native PSI complex to 107 mV in P700-F_X core. The decrease in the difference between $E_m(A_{1A})$ and $E_m(A_{1B})$ by 48 mV relative to the native PSI complex can be assigned predominantly to an up-shift of 34 mV in $E_m(A_{1B})$ as compared to a down-shift of only 14 mV in $E_m(A_{1A})$ (Ishikita et al., 2006).

6.2.3. Shift of $E_m(F_X)$ upon F_X-P700 core treatment

From the optical spectrum, the shift of $E_m(F_X)$ in urea treated PSI was measured to be +60mV (Parrett et al., 1989). Simply by using the atomic coordinates of the crystal structure of the native PSI complex for the remaining subunits of the P700-F_X core, we obtained the up-shift of 42 mV in the $E_m(F_X)$ relative to the native PSI complex (Ishikita et al., 2006). This implies that possible structural changes in the P700-F_X core that are induced by urea treatment are either small or not significant for the $E_m(F_X)$, which justifies the structural model for the P700-F_X core used in our computation (Ishikita et al., 2006).

We calculated the "direct contribution" of different residues/cofactors on $E_m(F_X)$ in the native PSI complex. Here, the negatively charged F_A and F_B are responsible for down-shifts of the $E_m(F_X)$ in the native PSI complex, by 110 mV and 34 mV, respectively. Due to the additivity of the direct contributions, these contributions to the $E_m(F_X)$ yield a total down-shift of 144 mV in the native PSI complex. Thus, elimination of atomic charges on both F_A and F_B from the native PSI complex should up-shift the $E_m(F_X)$ by 144 mV (Figure 6-2-1). However, in the native PSI complex, protein charges in the PsaC, PsaD and PsaE subunits essentially neutralize the down-shift of $E_m(F_X)$ caused by the presence of $F_{A/B}$, with an up-shift of 112 mV, contributed predominantly

by an up-shift of 90 mV from PsaC (Figure 6-2-1). Thus, the total direct influence of the charges on PsaC with $F_{A/B}$, PsaD and PsaE on $E_m(F_X)$ amounts to a down-shift of only –32 mV.

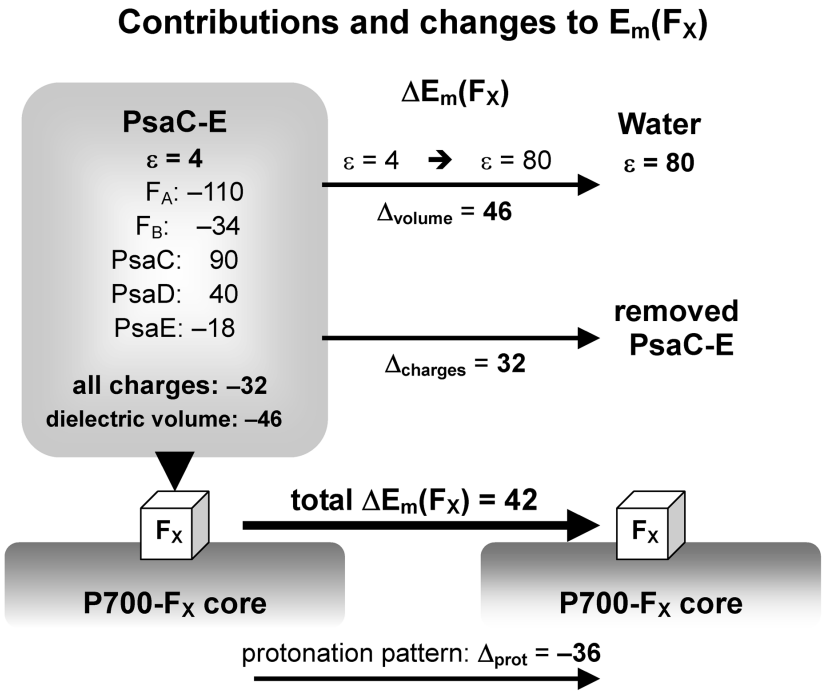

Figure 6-2-1. Direct influence on the shift of $E_m(F_X)$ from F_A, F_B and PsaC, PsaD, PsaE (PsaC-E) charges ($\Delta_{charges}$) and from dielectric volume (Δ_{volume}) by changing from the native PSI to the P700-F_X core. Calculated contributions and shifts (Δ) to $E_m(F_X)$ are given in units of mV. Contributions to $E_m(F_X)$ from specific components of the PsaC-E subunits are given in the left box that schematically represents these subunits. Changes (shifts) in $E_m(F_X)$ upon removal of the PsaC-E subunits are denoted by Δ. The total shift is given as sum of shifts from all charges, volume and changes in the protonation pattern associated with them, i.e. $\Delta E_m(F_X) = \Delta_{charges} + \Delta_{volume} + \Delta_{prot}$. The direct influence from dielectric volume is obtained if for vanishing charges in the PsaC-E subunits the protein dielectric volume of PsaC-E with $\varepsilon_P = 4$ is removed resulting in water occupancy with $\varepsilon_W = 80$. The indirect influence due to associated changes in the protonation pattern of titratable residues (Δ_{prot}) upon the removal of these subunits and $F_{A/B}$ is given for the charges and the dielectric volume of all three removed subunits.

Removal of the subunits and cofactors from the native PSI complex is also accompanied by exposure of the resulting P700-F_X core to bulk water. Creation of a new protein surface is often accompanied by a change of protonation pattern of nearby titratable residues. The change of protonation pattern from the native PSI complex to the P700-F_X core, though it is subtle, results in a down-shift of $E_m(F_X)$ by 36 mV (Figure 6-2-1). Therefore, the total influence on the shift of $E_m(F_X)$ in P700-F_X core, originating from the replacement of the protein volume of PsaC by water, yields an up-shift of only 10 mV with respect to the native PSI complex. Together with the up-shift of 32 mV obtained by the removal of the atomic charges from the subunits and of $F_{A/B}$ to generate P700-F_X, $E_m(F_X)$ in P700-F_X core is by 42 mV higher than that in the native PSI complex.

Conclusion:

Based on this simple model for the P_{700}-F_X core structure by the removal of subunits PsaC, PsaD and PsaD, **we can reproduce** (Ishikita et al., 2006) **the measured shift of**

$E_m(F_X)$ (Parrett et al., 1989) **and, as a consequence, obtain an acceleration of ET from A_1 to F_X as observed in the kinetic measurements** (Gong et al., 2003) **for urea treated PSI.** Thus, this simple model for the P700-F_X core based on the native PSI complex can essentially explain the experimental results.

6.3. Difference between $E_m(A_1)$ of PSI and $E_m(Q)$ of PSII and bRC.

It is still an open question why the $E_m(A_{1A/B})$ in PSI is so extremely negative (–690 - –530 mV (Ishikita and Knapp, 2003)) relative to the $E_m(Q_{A/B})$ in bRC (–180 - –100 mV (Prince and Dutton, 1976; Arata and Parson, 1981; Ishikita et al., 2003; Ishikita and Knapp, 2004)) and in PSII (–100 - +50 mV (Krieger et al., 1995; Ishikita and Knapp, 2005e)). This E_m difference is not merely due to the difference in E_m of –463 mV (in DMF (Prince et al., 1983)) for phylloquinone of PSI, –360 mV (in DMF (Prince et al., 1983)) for ubiquinone of bRC and –369 mV (in DMF (Prince et al., 1986)) for plastoquinone of PSII (see Figure 6-3-1).

6.3.1. H-bond pattern for quinones

In PSI, only one of the two carbonyl oxygen of the quinones are H-bonded with the backbone amide groups (Leu-A722 to A_{1A} (N – O distance 2.7 Å) and Leu-B706 to A_{1B} (N – O distance 2.8 Å) (Jordan et al., 2001)). Ser-A692/ Ser-B672 is at H-bond distance to $A_{1A/B}$ (O – O distances 3.3/ 3.4 Å) (Figure 6-1-1). However, these residues do not form H bonds with A_1 due to unfavorable H-bond angles. On the other hand, both carbonyl oxygens of $Q_{A/B}$ in bRC (Stowell et al., 1997) and PSII (Ferreira et al., 2004) are H bonded. Therefore, the difference of H-bond pattern for quinones between PSI and bRC/PSII is speculated to be one of the factors to differentiate between $E_m(A_{1A/B})$ and $E_m(Q_{A/B})$ (reviewed in ref. (Brettel and Leibl, 2001)). To test this assumption, we rotated the hydroxyl groups of Ser-A692/ Ser-B672 to form an H bond with $A_{1A/B}$, and calculated the $E_m(A_{1A/B})$ in the presence of this virtual H bond between the Ser residues and A_1. The resulting up-shift of the $E_m(A_{1A/B})$ was at most ~70 mV (Ishikita and Knapp, 2003). This value is not sufficiently large to account for the net E_m difference of quinones between PSI and bRC/PSII.

6.3.2. Fe_4S_4 center F_X in PSI and the Fe-complex in bRC/PSII

In our computation, the E_m of quinones is up-shifted by 190–270 mV in bRC from *Rb. sphaeroides* with respect to that in DMF (Ishikita et al., 2003; Ishikita and Knapp, 2004), but down-shifted by 86–223 mV in PSI (Ishikita and Knapp, 2003). Previously, we revealed that in the light-exposed structure of bRC from *Rb. sphaeroides*, the net unit positive charge of the Fe-complex is responsible for a strong up-shift of the $E_m(Q_{A/B})$ by ~170 mV for Q_A (Ishikita and Knapp, 2003) and for Q_B (Ishikita et al., 2003). Near A_1 in PSI is the Fe_4S_4 center, F_X. The net charge of the Fe-complex and F_X are significantly different, being +1 for the former (including Glu ligand) and –2 for the latter (as $[Fe_4S_4(SCH_3)_4]^{2-}$). In our computation, the direct influence of the F_X charge is calculated to provide down-shifts of 237 mV and 256 mV for $E_m(A_{1A})$ and $E_m(A_{1B})$, respectively (Ishikita and Knapp, 2003).

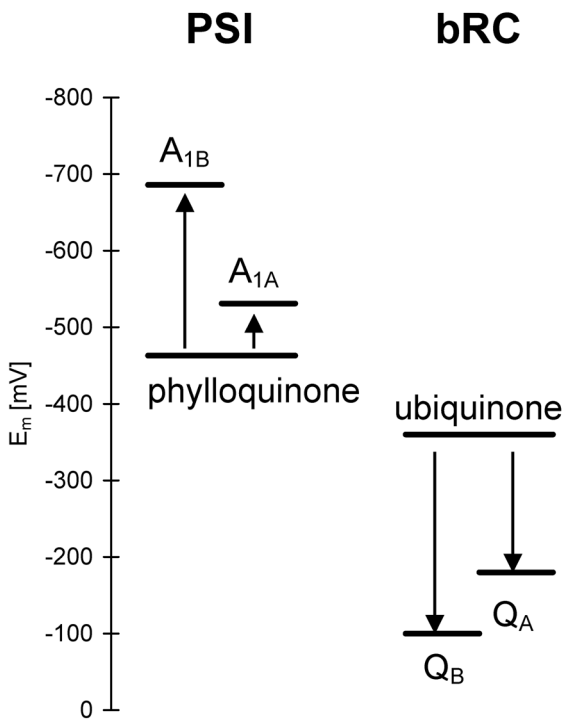

Figure 6-3-1. Comparison of the Em for quinone in solution (DMF) with that calculated in PSI and bRC.

Conclusion:

The large $E_m(Q_{A/B})$ difference in bRC and PSII relative to $E_m(A_{1A/B})$ in PSI is mostly due to the **charge difference between the Fe-complex in the former and the F_X in the latter, which yields an E_m difference of ~410-430 mV. An additional ~70 mV difference can be explained by the absence of the second H bond to A_1 in PSI** (Ishikita and Knapp, 2003)**.**